

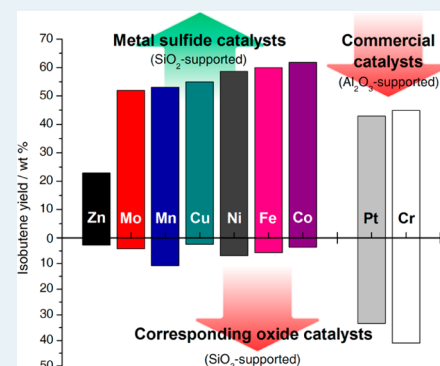
# Highly Efficient Metal Sulfide Catalysts for Selective Dehydrogenation of Isobutane to Isobutene

Guowei Wang, Chunyi Li,\* and Honghong Shan

State Key Laboratory of Heavy Oil Processing, China University of Petroleum, Qingdao 266580, People's R China

## Supporting Information

**ABSTRACT:** Metal sulfide catalysts were highly efficient in the activation of C–H bond for isobutane dehydrogenation, and the dehydrogenation performance was better than that of the commercial catalysts  $\text{Cr}_2\text{O}_3/\text{Al}_2\text{O}_3$  and  $\text{Pt-Sn}/\text{Al}_2\text{O}_3$ , providing a class of environmentally friendly and economical alternative catalysts for industrial application.



**KEYWORDS:** isobutane, dehydrogenation, isobutene, metal sulfide, sulfidation

With increasing demand for isobutene, a widely utilized raw material for the synthesis of polymers<sup>1</sup> and octane-boosting additives in gasoline,<sup>2</sup> isobutane dehydrogenation has drawn extensive attention in recent years.  $\text{CrO}_x$ <sup>3–5</sup> and Pt-based catalysts<sup>6–8</sup> are known to be two typical catalysts applied in the catalytic dehydrogenation of isobutane on a commercial scale for decades. Although the catalytic performance of these catalysts is relatively satisfactory, the harmful impacts of Cr and the high cost of Pt have limited their application to some extent. Moreover, even with extensive research<sup>9–12</sup> focused on alternative routes, that is, oxidative dehydrogenation, it is still hard to control the extent of oxidation, which inevitably leads to an increase in the formation of  $\text{CO}_x$  and decrease in the selectivity toward olefins.<sup>13,14</sup> Therefore, the major challenge in dehydrogenation technology is to develop a new type of catalyst with environmentally friendly and cost-effective characteristics as well as excellent performance in the absence of oxidants.<sup>15</sup>

To achieve this goal, many attempts have been made. However, when Co and Ni were evaluated as active components, a great amount of methane was generated. According to the literature,<sup>16–18</sup> the dissociation energy of C–C bonds is smaller than that of C–H bonds; therefore, the active species preferentially insert into C–C bonds, and cracking reactions occur as a result. Georgiadis et al.<sup>19</sup> also held the point that, for both Co and Ni, demethanation is preferred over dehydrogenation on energetic grounds. Consequently, certain methods should be carried out to suppress the undesired C–C bond cleavage and selectively activate the C–H bond of the alkane molecules.

Molybdenum sulfide-alumina catalyst was found to be efficient in paraffin dehydrogenation with CO as a hydrogen

acceptor as early as 1966.<sup>20</sup> In 1994, Resasco et al.<sup>21</sup> treated a  $\text{Ni}/\text{Al}_2\text{O}_3$  catalyst with dimethyl sulfoxide and observed that an increased selectivity toward isobutene and a decreased coke formation rate, as well as an isobutene yield of 21%, could be achieved. Although the secondary reactions were effectively inhibited after the modification, the catalyst activity still needed to be improved. Moreover, Kobayashi and Shimizu<sup>22</sup> also reported similar promoting effect of sulfur on isobutane dehydrogenation over a Pt-alkali metal/ $\text{Al}_2\text{O}_3$  catalyst.

Supported metal sulfide catalysts, for example,  $\text{MoS}_2$ ,<sup>23</sup>  $\text{CoS}$ ,<sup>24</sup> and  $\text{NiS}$ ,<sup>25</sup> have been widely applied in hydrogenation processes for years. Hydrogenation and dehydrogenation are reverse reactions; therefore, the questions to be answered are why sulfide catalysts have not been applied in dehydrogenation processes, and whether metal sulfides are able to catalyze dehydrogenation reactions. Recently, we have found that  $\text{MgAl}_2\text{O}_4$ -supported  $\text{NiS}$  catalysts exhibited excellent performance in isobutane dehydrogenation<sup>26</sup> and applied for patents.<sup>27,28</sup> Then, how about other metal sulfides?

In this paper, to investigate and compare the performance of various metal sulfides, inert silica was chosen as the support. A variety of metal oxides, including  $\text{ZnO}$ ,  $\text{CuO}$ ,  $\text{MnO}_2$ ,  $\text{MoO}_3$ ,  $\text{Fe}_2\text{O}_3$ ,  $\text{Co}_3\text{O}_4$ , and  $\text{NiO}$  (some even with inferior hydrogenation activity, e.g.,  $\text{ZnO}$ ,  $\text{CuO}$  and  $\text{MnO}_2$ ), all environmentally friendly and inexpensive, with 13 wt % loading supported on silica were prepared and pretreated in  $\text{H}_2\text{S}/\text{H}_2$  flow. Afterward, all these sulfided catalysts were evaluated and

Received: November 18, 2013

Revised: March 1, 2014

Published: March 5, 2014

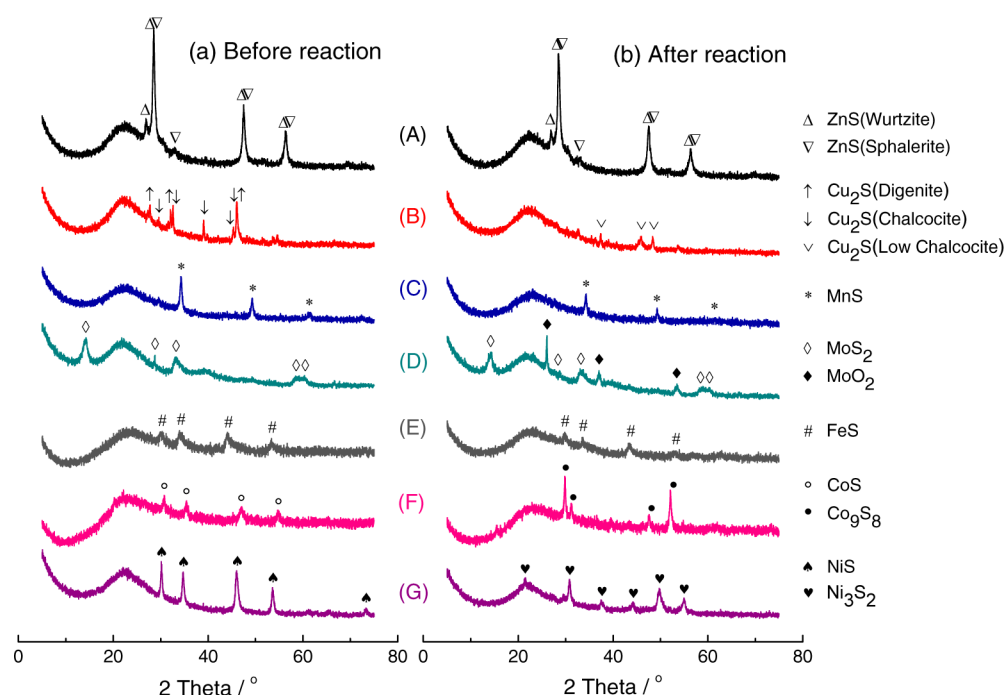


**Figure 1.** XRD patterns of sulfided SiO<sub>2</sub>-supported oxide catalysts before (a) and after (b) reaction: (A) ZnO/SiO<sub>2</sub>, (B) CuO/SiO<sub>2</sub>, (C) MnO<sub>2</sub>/SiO<sub>2</sub>, (D) MoO<sub>3</sub>/SiO<sub>2</sub>, (E) Fe<sub>2</sub>O<sub>3</sub>/SiO<sub>2</sub>, (F) Co<sub>3</sub>O<sub>4</sub>/SiO<sub>2</sub>, and (G) NiO/SiO<sub>2</sub>.

**Table 1. Physicochemical Properties and Catalytic Performance of SiO<sub>2</sub>-Supported Metal Oxide and Corresponding Metal Sulfide Catalysts for Isobutane Dehydrogenation<sup>a</sup>**

	oxide catalysts				sulfide catalysts			
	S <sub>BET</sub> , m <sup>2</sup> /g	V <sub>p</sub> , cm <sup>3</sup> /g	C <sub>isobutane</sub> <sup>b</sup> , wt %	S <sub>isobutene</sub> <sup>c</sup> , wt %	S <sub>BET</sub> , m <sup>2</sup> /g	V <sub>p</sub> , cm <sup>3</sup> /g	C <sub>isobutane</sub> <sup>b</sup> , wt %	S <sub>isobutene</sub> <sup>c</sup> , wt %
ZnO/SiO <sub>2</sub>	252	1.01	4.2	66.9	249	0.98	28.4	80.6
CuO/SiO <sub>2</sub>	248	0.97	3.7	68.6	244	0.93	64.9	84.7
MnO <sub>2</sub> /SiO <sub>2</sub>	245	0.91	19.1	56.6	240	0.87	62.8	84.5
MoO <sub>3</sub> /SiO <sub>2</sub>	234	0.87	6.4	66.4	229	0.81	65.2	79.8
Fe <sub>2</sub> O <sub>3</sub> /SiO <sub>2</sub>	239	0.88	13.3	43.5	236	0.84	69.2	86.6
Co <sub>3</sub> O <sub>4</sub> /SiO <sub>2</sub>	225	0.86	14.1	25.3	211	0.71	71.1	87.0
NiO/SiO <sub>2</sub>	236	0.88	91.1	7.6	234	0.74	67.0	87.6

<sup>a</sup>Reaction conditions: temp, 560 °C; 4 g of catalyst loaded; 14.3 vol % *i*-C<sub>4</sub>H<sub>10</sub> in nitrogen at a total flow rate of 14 mL min<sup>-1</sup>. <sup>b</sup>Conversion of isobutane. <sup>c</sup>Selectivity to isobutene, and all the data were obtained at the very beginning of the reaction.

characterized. Moreover, a detailed catalyst preparation procedure is provided in the Supporting Information.

XRD patterns of these sulfided SiO<sub>2</sub>-supported oxide catalysts are shown in Figure 1a. Diffraction peaks marked with certain symbols represent corresponding metal sulfides. As for the sulfided ZnO/SiO<sub>2</sub> catalyst, ZnS was detected on the catalyst surface in the form of both wurtzite and sphalerite. Moreover, two forms of Cu<sub>2</sub>S existing on the surface of the sulfided CuO/SiO<sub>2</sub> catalyst are chalcocite and digenite. In brief, all the oxides on the investigated catalysts were effectively converted to the corresponding sulfides after sulfidation treatment. From A to G, the corresponding sulfides were ZnS, Cu<sub>2</sub>S, MnS, MoS<sub>2</sub>, FeS, CoS, and NiS.

Table 1 compares the physicochemical properties and dehydrogenation performance of SiO<sub>2</sub>-supported metal oxide and corresponding sulfide catalysts. The surface area of all the oxide catalysts was larger than 220 m<sup>2</sup>/g, and the pore volume was in a range between 0.86 and 1.01 cm<sup>3</sup>/g. Although both surface area and pore volume of the catalysts decreased slightly after sulfidation, the sulfidation treatment has no obvious negative effect on the pore structure of the catalyst in general.

Isobutane conversion and isobutene selectivity of the oxide catalysts behaved in opposite ways, as reflected by the results that NiO/SiO<sub>2</sub>, with the highest isobutane conversion, presented the lowest selectivity to isobutene, whereas CuO/SiO<sub>2</sub> with the lowest conversion, exhibited the highest selectivity. As for the Co and Ni-based catalysts, the generation of a large amount of methane was indicative of high activity for C–C bond breaking. Surprisingly, after sulfidation with H<sub>2</sub>S/H<sub>2</sub>, all the catalysts but NiO/SiO<sub>2</sub> exhibited significantly improved isobutane conversion. Meanwhile, the selectivity toward isobutene was basically higher than 80 wt % for all catalysts, demonstrating the highly efficient activation ability of C–H bond for the sulfided catalysts. Most importantly, in addition to Mo, Ni, and Co, widely applied in hydrogenation processes, the other metals rarely used in hydrogenation reaction also exhibited improved dehydrogenation performance after sulfidation with H<sub>2</sub>S/H<sub>2</sub>. Furthermore, detailed product distributions of isobutane dehydrogenation over NiO/SiO<sub>2</sub> catalyst before and after sulfidation are listed in Table S1 in the Supporting Information.

For comparison, the industrially relevant catalysts  $\text{Cr}_2\text{O}_3/\text{Al}_2\text{O}_3$  and  $\text{Pt-Sn}/\text{Al}_2\text{O}_3$  were prepared according to the literature,<sup>29,30</sup> and their dehydrogenation performance was evaluated under the same reaction conditions. As listed in Table 2, both catalysts were less active in dehydrogenation than most

**Table 2. Catalytic Performance of Commercial Relevant  $\text{Cr}_2\text{O}_3$  and Pt-Based Catalysts for Isobutane Dehydrogenation<sup>a</sup>**

	$C_{\text{isobutane}}^b$ , wt %	$S_{\text{isobutene}}^c$ , wt %
$\text{Cr}_2\text{O}_3/\text{Al}_2\text{O}_3^d$	54.5	82.4
$\text{Pt-Sn}/\text{Al}_2\text{O}_3^e$	49.7	86.2
$\text{Cr}_2\text{O}_3/\text{SiO}_2^f$	48.4	84.9
$\text{Pt}/\text{SiO}_2^g$	42.7	78.1

<sup>a</sup>Reaction conditions: temp, 560 °C; 4 g of catalyst loaded; 14.3 vol %  $i\text{-C}_4\text{H}_{10}$  in nitrogen at a total flow rate of 14 mL  $\text{min}^{-1}$ . <sup>b</sup>Conversion of isobutane. <sup>c</sup>Selectivity to isobutene, and all the data were obtained at very beginning of the reaction. <sup>d</sup>Containing 15 wt %  $\text{Cr}_2\text{O}_3$ . <sup>e</sup>Containing 0.5 wt % Pt and 1.5 wt % Sn. <sup>f</sup>Containing 13 wt %  $\text{Cr}_2\text{O}_3$ . <sup>g</sup>Containing 13 wt % Pt.

of the sulfide catalysts. The isobutene yield decreased in the following order:  $\text{CoS}/\text{SiO}_2 > \text{FeS}/\text{SiO}_2 > \text{NiS}/\text{SiO}_2 > \text{Cu}_2\text{S}/\text{SiO}_2 > \text{MnS}/\text{SiO}_2 > \text{MoS}_2/\text{SiO}_2 > \text{Cr}_2\text{O}_3/\text{Al}_2\text{O}_3 > \text{Pt-Sn}/\text{Al}_2\text{O}_3 > \text{ZnS}/\text{SiO}_2$ . The isobutene yield and isobutene selectivity versus conversion curves for all tested catalysts are compared in Figure S1 in the Supporting Information.

To exclude the effects of metal content and support, 13Pt/ $\text{SiO}_2$  and 13 $\text{Cr}_2\text{O}_3/\text{SiO}_2$  catalysts were prepared and evaluated in isobutane dehydrogenation, with the results integrated in Table 2. The dehydrogenation performance was not better than that of  $\text{Cr}_2\text{O}_3/\text{Al}_2\text{O}_3$  and  $\text{Pt-Sn}/\text{Al}_2\text{O}_3$  catalysts, which probably resulted from the weak interaction between the silica support and active component. Moreover, the aggregation of Pt on 13Pt/ $\text{SiO}_2$  catalyst could also contribute to the unsatisfactory dehydrogenation performance.

Moreover, when  $\text{Al}_2\text{O}_3$  and  $\text{MgAl}_2\text{O}_4$  were taken as supports of metal sulfide catalysts, similarly high levels of isobutane conversion and isobutene selectivity could be achieved (see Supporting Information (SI) Figure S2), demonstrating that the excellent performance of metal sulfides has little to do with the support.

On the basis of the above discussions, the metal sulfides (detected by XRD) were probably responsible for the significantly improved dehydrogenation performance. Moreover, according to the literature, sulfur adsorbed at the kinked edges of the Pt catalysts substantially deactivated cracking sites<sup>31</sup> and inhibited C–C bond breaking.<sup>32</sup> Therefore, one possible explanation is that, with the introduction of sulfur, the steric hindrance of the metal–sulfur bond hindered the interaction between the carbon atoms of isobutane molecule and the metal sites active for C–C bond cleavage and, consequently, led to limited cracking reactions and improved dehydrogenation performance.

Although the dehydrogenation performance was improved remarkably after sulfidation, the catalytic activity of the metal sulfide catalysts was much less stable than that of the commercial catalysts (see Figure 2). Taking the sulfided NiO/ $\text{SiO}_2$  catalyst as an example (see SI Figure S3a), the decreased dehydrogenation activity was probably caused by the change in the active sites. Figure 1b illustrates the XRD patterns of  $\text{SiO}_2$ -supported metal sulfide catalysts reacted for 8 h, which

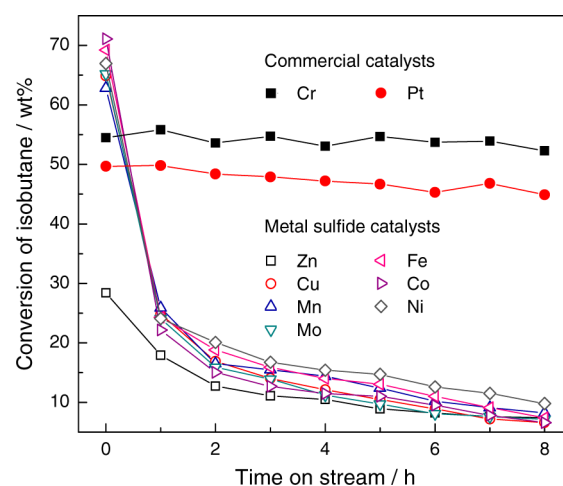


**Figure 2.** Catalytic activity of metal sulfide catalysts and commercial relevant catalysts for isobutane dehydrogenation.

exhibited relatively low catalytic activity (see SI Table S2). For  $\text{ZnS}/\text{SiO}_2$ ,  $\text{MnS}/\text{SiO}_2$ ,  $\text{MoS}_2/\text{SiO}_2$ , and  $\text{FeS}/\text{SiO}_2$  catalysts after reaction, the intensity of the diffraction peaks corresponding to metal sulfides decreased significantly. In addition,  $\text{MoO}_2$  was also detected on  $\text{MoS}_2/\text{SiO}_2$  catalyst after reaction, indicating the loss of sulfur species. As for the  $\text{Cu}_2\text{S}/\text{SiO}_2$  catalyst, low chalcocite, another form of  $\text{Cu}_2\text{S}$ , appeared in much lower intensity after reaction. Moreover, accompanied by the disappearance of CoS and NiS,  $\text{Co}_9\text{S}_8$  and  $\text{Ni}_3\text{S}_2$  emerged on the  $\text{CoS}/\text{SiO}_2$  and  $\text{NiS}/\text{SiO}_2$  catalysts after reaction, respectively. In summary, although the pathways of sulfur loss were different for these sulfide catalysts, realized by either the decrease in the amount of original metal sulfides or the formation of new compounds with less sulfur content, the loss of sulfur was probably the primary reason for the deactivation of the catalysts. To quantify the sulfur content on sulfided catalysts, elemental analysis measurement has been carried out. Sulfur contents of the fresh sulfided NiO/ $\text{SiO}_2$  catalyst and the catalysts after 1 and 8 h of reaction were 5.38, 5.11, and 3.43 wt %, respectively, directly reflecting the sulfur loss from the catalyst during the reaction.

To further determine the variations of surface sulfur species during the reaction, XPS characterization was performed over sulfided NiO/ $\text{SiO}_2$  catalysts before and after reaction. The S 2p XPS spectra are illustrated in SI Figure S4. For the sulfided catalysts before reaction, observation of the doublet characteristic of  $\text{S}^{2-}$  species directly supported that the metal oxides on the catalysts were converted to the corresponding sulfides after sulfidation treatment. After 8 h of reaction, the intensity of the  $\text{S}^{2-}$  doublet decreased greatly. For the Ni 2p XPS spectra shown in SI Figure S5, a characteristic peak at 852.4 eV represents the presence of NiS, and the intensity of this peak decreased after reaction, which is consistent with the results of S 2p XPS spectra. Such observation further proved the consumption of metal sulfide during the reaction.

Furthermore, an online mass spectrometer was applied to detect the released gases during isobutane dehydrogenation over the sulfided catalysts. For the sulfided NiO/ $\text{SiO}_2$  catalyst, in addition to isobutane and the main products (including hydrogen and isobutene), hydrogen sulfide was also detected (see SI Figure S6), indicating that sulfur was lost mainly in the form of hydrogen sulfide. Complete mass balance calculation of the reaction has also been conducted, with the results listed in

Table S3 in the Supporting Information. As listed in the table, the sulfur mass balance and overall mass balance reached up to 98 and 97 wt %, respectively. Moreover, the mass balance data indicated that the reaction was not a stoichiometric reaction. If the reaction occurred in a stoichiometric way, that is,  $\text{NiS} + i\text{-C}_4\text{H}_{10} \rightarrow i\text{-C}_4\text{H}_8 + \text{H}_2\text{S} + \text{Ni}$ , only 0.019 g of isobutane could be converted according to the sulfur loss weight of the catalyst (0.0108 g). However, the reacted isobutane (0.181 g) was much more than that amount, so it could be concluded that the reaction was not stoichiometric, and the catalyst served more like a catalyst rather than the reactant.

To recover the catalyst activity, the spent NiS/SiO<sub>2</sub> catalyst was sulfided by H<sub>2</sub>S/H<sub>2</sub> for another 3 h after 8 h reaction, and in total, five sulfidation–reaction cycles were conducted. Within the five cycles, the initial isobutane conversion was maintained at a relatively steady level (see SI Figure S3b), that is, the catalyst activity could be fully recovered after every sulfidation treatment. In practice, to reduce cost, coproduced sulfur-containing dry gas can be used to replace H<sub>2</sub>S to treat the catalyst in the sulfidation process.

To deepen the understanding of catalyst deactivation, isobutane dehydrogenation over sulfided NiO/SiO<sub>2</sub> catalyst under a cofeed of H<sub>2</sub>S (2 mL/min) has been further carried out, and the results are illustrated in Figure S7 in the Supporting Information. It can be observed that both isobutane conversion and isobutene selectivity decreased to some extent in the initial 2 h. The catalytic performance remained relatively steady afterward, with isobutene yield up to 50 wt %, which was indicative of improved catalyst stability under the cofeed of H<sub>2</sub>S. Meanwhile, a small quantity of sulfided hydrocarbons, including methanethiol, ethanethiol, and thiophen, were generated during the reaction.

It should also be mentioned that a small amount of coke (0.15 wt % for the spent NiS/SiO<sub>2</sub> catalyst after 8 h reaction) was accumulated on the catalyst during the continuous reaction process, which also contributed to the catalyst deactivation to some extent. However, it was fortunate that the treatment with H<sub>2</sub>S/H<sub>2</sub> could eliminate most of the deposited coke at the reaction temperature of 560 °C, as evidenced by the H<sub>2</sub>-TPR-MS profile of the spent NiS/SiO<sub>2</sub> catalyst illustrated in SI Figure S8, which demonstrated the removal of coke in the form of methane under hydrogen atmosphere. Given that the sulfur loss and coke deposition occurred simultaneously during the reaction, to achieve continuous operation, a circulating fluidized bed reactor equipped with a dehydrogenation reactor, it is suggested that a regenerator for coke burning and a sulfidation section be employed in future industrial application. However, the coke deposited on the catalyst during isobutane dehydrogenation was low, and the heat released from coke burning is not sufficient for the reaction. Therefore, an appropriate fuel (e.g., coproduced dry gas) can be introduced and burned in the regenerator to supply extra heat and achieve heat balance.

In conclusion, metal sulfide catalysts, a novel class of nonnoble metal catalysts for alkane dehydrogenation, exhibited relatively satisfactory dehydrogenation performance with improved activation ability of the C–H bond over the C–C bond. In addition to the active components, such as Mo, Ni, and Co widely applied in hydrogenation processes, the sulfides of Cu, Mn, and Fe, barely reported in hydrogenation reactions, also showed excellent performance. Under the same operating conditions, the performance of these catalysts was even better than that of the industrial Cr<sub>2</sub>O<sub>3</sub>/Al<sub>2</sub>O<sub>3</sub> and Pt–Sn/Al<sub>2</sub>O<sub>3</sub>

catalysts. Nevertheless, possible sulfur loss occurs during the application of these catalysts, and therefore, measures for sulfur replenishment should be implemented.

## ■ ASSOCIATED CONTENT

### Supporting Information

Further details are given in Figures S1 to S8 and Tables S1 to S3. This material is available free of charge via the Internet at <http://pubs.acs.org>.

## ■ AUTHOR INFORMATION

### Corresponding Author

\*E-mail: [chyli@upc.edu.cn](mailto:chyli@upc.edu.cn), [chyli\\_upc@126.com](mailto:chyli_upc@126.com).

### Notes

The authors declare no competing financial interest.

## ■ ACKNOWLEDGMENTS

This work was financially supported by the National Natural Science Foundation of China (No. U1362201), the National 973 Program of China (No. 2012CB215006), and the Fundamental Research Funds for the Central Universities (No. 12CX06040A).

## ■ REFERENCES

- (1) Xie, H.; Wu, Z.; Overbury, S. H.; Liang, C.; Schwartz, V. J. *Catal.* **2009**, *267*, 158–166.
- (2) Centeno, M. A.; Debois, M.; Grange, P. *J. Catal.* **2000**, *192*, 296–306.
- (3) Zimmermann, H.; Versluis, F. U.S. Patent 5378350, 1995.
- (4) Buonomo, F.; Jezzi, R.; Notari, B.; Kotelnikov, G. R.; Michailov, K. R.; Patanov, V. A. U.S. Patent 4746643, 1988.
- (5) Fritz, P. M.; Boelt, H. V.; Hackner, H.; Van, D. G. J. EP. Patent 0947247, 1999.
- (6) Iezzi, R.; Buonomo, F.; Sanfilippo, D. U.S. Patent 5143886, 1992.
- (7) Herber, R. R.; Thompson, G. J. U.S. Patent 4806624, 1989.
- (8) Olbrich, M. E.; McKay, D. L.; Montgomery, D. P.; Jean, B. U.S. Patent 4926005, 1990.
- (9) Li, J.; Wang, C.; Huang, C.; Sun, Y.; Weng, W.; Wan, H. *Appl. Catal., A* **2010**, *382*, 99–105.
- (10) Schimmoeller, B.; Jiang, Y.; Pratsinis, S. E.; Baiker, A. *J. Catal.* **2010**, *274*, 64–75.
- (11) Troțuș, I.-T.; Teodorescu, C. M.; Pârvulescu, V. I.; Marcu, I.-C. *ChemCatChem* **2013**, *5*, 757–765.
- (12) Siahvashi, A.; Chesterfield, D.; Adesina, A. A. *Ind. Eng. Chem. Res.* **2013**, *52*, 4017–4026.
- (13) Zhang, Q.; Cao, C.; Xu, T.; Sun, M.; Zhang, J.; Wang, Y.; Wan, H. *Chem. Commun.* **2009**, *45*, 2376–2378.
- (14) Wang, H.; Cong, Y.; Yang, W. *Chem. Commun.* **2002**, *38*, 1468–1469.
- (15) Wang, G.; Li, C.; Shan, H.; Wu, W. *Ind. Eng. Chem. Res.* **2013**, *52*, 13297–13304.
- (16) Halle, L.; Houriet, R.; Kappes, M. M.; Staley, R. H.; Beauchamp, J. *J. Am. Chem. Soc.* **1982**, *104*, 6293–6297.
- (17) Blomberg, M. R. A.; Siegbahn, P. E. M.; Nagashima, U.; Wennerberg, J. *J. Am. Chem. Soc.* **1991**, *113*, 424–433.
- (18) Jacobson, D.; Freiser, B. *J. Am. Chem. Soc.* **1983**, *105*, 5197–5206.
- (19) Georgiadis, R.; Fisher, E. R.; Armentrout, P. *J. Am. Chem. Soc.* **1989**, *111*, 4251–4262.
- (20) Hepp, H. J.; Johnson, M. M. U.S. Patent 3280210, 1966.
- (21) Resasco, D. E.; Marcus, B. K.; Huang, C. S.; Durante, V. A. *J. Catal.* **1994**, *146*, 40–55.
- (22) Kobayashi, J.; Shimizu, T. *Bull. Chem. Soc. Jpn.* **2000**, *73*, 759–763.
- (23) Skrabalak, S. E.; Suslick, K. S. *J. Am. Chem. Soc.* **2005**, *127*, 9990–9991.

- (24) Dhas, N. A.; Ekhtiarzadeh, A.; Suslick, K. S. *J. Am. Chem. Soc.* **2001**, *123*, 8310–8316.
- (25) Zhang, L.; Yu, J. C.; Mo, M.; Wu, L.; Li, Q.; Kwong, K. W. *J. Am. Chem. Soc.* **2004**, *126*, 8116–8117.
- (26) Wang, G.; Meng, Z.; Liu, J.; Li, C.; Shan, H. *ACS Catal.* **2013**, *3*, 2992–3001.
- (27) Li, C.; Wang, G.; Sun, N.; Sun, Y. C.N. Patent 201210536414.7, 2012.
- (28) Li, C.; Wang, G.; Sun, N.; Sun, Y. C.N. Patent 201310014789.1, 2013.
- (29) Weckhuysen, B. M.; Schoonheydt, R. A. *Catal. Today* **1999**, *51*, 223–232.
- (30) Iglesias-Juez, A.; Beale, A. M.; Maaijen, K.; Weng, T. C.; Glatzel, P.; Weckhuysen, B. M. *J. Catal.* **2010**, *276*, 268–279.
- (31) Coughlin, R. W.; Hasan, A.; Kawakami, K. *J. Catal.* **1984**, *88*, 163–176.
- (32) Somorjai, G. A.; Li, Y. *Introduction to Surface Chemistry and Catalysis*; Wiley: Hoboken, NJ, 2010.